THE JOURNAL OF BIOLOGICAL CHEMISTRY VOL. 286, NO. 26, pp. 23012–23021, July 1, 2011

Phospholipase Cε Scaffolds to Muscle-specific A Kinase Anchoring Protein (mAKAPβ) and Integrates Multiple Hypertrophic Stimuli in Cardiac Myocytes*[S]

Received for publication, February 16, 2011, and in revised form, April 11, 2011 Published, JBC Papers in Press, May 5, 2011, DOI 10.1074/jbc.M111.231993

Lianghui Zhang[‡1], **Sundeep Malik**[‡1], **Grant G. Kelley**[§], **Michael S. Kapiloff**[¶], **and Alan V. Smrcka**[‡‖2]

From the [‡]*Department of Pharmacology and Physiology and the* [‖]*Aab Institute of Cardiovascular Science, University of Rochester School of Medicine and Dentistry, Rochester, New York 14642, the* [§]*Department of Hospital Medicine, Saint Joseph's Hospital Health Center, Syracuse, New York 13203, and the* [¶]*Departments of Medicine and Pediatrics, Interdisciplinary Stem Cell Institute, University of Miami Miller School of Medicine, Miami, Florida 33101*

To define a role for phospholipase Cε (PLCε) signaling in cardiac myocyte hypertrophic growth, PLCε protein was depleted from neonatal rat ventricular myocytes (NRVMs) using siRNA. NRVMs with PLCε depletion were stimulated with endothelin (ET-1), norepinephrine, insulin-like growth factor-1 (IGF-1), or isoproterenol and assessed for development of hypertrophy. PLCε depletion dramatically reduced hypertrophic growth and gene expression induced by all agonists tested. PLCε catalytic activity was required for hypertrophy development, yet PLCε depletion did not reduce global agonist-stimulated inositol phosphate production, suggesting a requirement for localized PLC activity. PLCε was found to be scaffolded to a muscle-specific A kinase anchoring protein (mAKAPβ) in heart and NRVMs, and mAKAPβ localizes to the nuclear envelope in NRVMs. PLCε-mAKAP interaction domains were defined and overexpressed to disrupt endogenous mAKAPβ-PLCε complexes in NRVMs, resulting in significantly reduced ET-1-dependent NRVM hypertrophy. We propose that PLCε integrates multiple upstream signaling pathways to generate local signals at the nucleus that regulate hypertrophy.

Pathologic hypertrophic growth of the myocardium, a process associated with the development of heart failure, occurs in response to various stimuli including pressure overload and chronic increases in circulating hormones that place long term stress on the heart. Many of these hormones act on receptors in cardiac myocytes including adrenergic and endothelin receptors to initiate hypertrophic signaling cascades (1–3). The exact participants in these hypertrophic signaling cascades have been the subject of intense investigation. One common signaling mechanism closely coupled to receptor activation is activation of phosphatidylinositol-specific phospholipase C (PLC)[3] (4). A role for PLC activity in regulation of hypertrophic signaling has been suggested because G_q, a potent stimulator of hypertrophy (5), directly stimulates PLCβ as a major regulatory pathway (6). Additionally, growth factors such as insulin-like growth factor-1 (IGF-1) that stimulate physiological hypertrophy activate PLCγ (7, 8). Recently, it has been reported that a splice variant of PLCβ, PLCβ1b, is required for hypertrophy downstream of α1-adrenergic receptor stimulation and suggested to be a major mediator of G_q-dependent cardiac hypertrophy (9).

The PLC family consists of 12 isoforms regulated by diverse upstream signal inputs, all of which hydrolyze phosphatidylinositol 4,5-bisphosphate to diacylglycerol (DAG) and inositol trisphosphate (IP_3) (10, 11). Although containing a common PLC catalytic core domain, PLCβ, PLCγ, PLCδ, and PLCε isoforms are very different in terms of overall domain structure and regulatory mechanisms, indicating that they are unlikely to play overlapping roles in the cells. PLCε is unique in that it is directly regulated by various small GTPases, including Ras, Rho, and Rap (12–16), and Gβγ subunits, but not $G\alpha_q$. PLCε has been shown to signal downstream of G protein-coupled receptors, including β-adrenergic receptors (βARs), lysophosphatidic acid and sphingosine 1-phophate receptors (EdgRs), protease-activated receptors (13, 17), and growth factor receptor tyrosine kinases, including PDGF receptors (15) and EGF receptors (13). Thus, PLCε is ideally positioned to integrate multiple signaling inputs in various cell types including cardiac myocytes.

Recent studies of $PLC\epsilon^{-/-}$ mice revealed alterations in βAR-dependent regulation of cardiac ionotropy and hypertrophy (18). These mice had no hypertrophy at baseline but developed greater hypertrophy than wild type animals in response to chronic isoproterenol treatment. Thus, PLCε appeared to protect mice from stimulus-induced cardiac hypertrophy. In wild type mice, the levels of PLCε mRNA and protein increase during pressure overload or chronic isoproterenol (Iso) treatment. PLCε RNA levels are elevated in biopsies from human heart failure samples. To explore a mechanistic role for PLCε in hypertrophy, we utilized an siRNA protocol in an established cellular model of cardiac hypertrophy, the neonatal rat ventric-

* This work was supported, in whole or in part, by National Institutes of Health Grants GM R01 053536 (to A. V. S.) and HL075398 (to M. S. K.).

[S] The on-line version of this article (available at http://www.jbc.org) contains supplemental Figs. 1–5.

[1] Both authors contributed equally to this work.

[2] To whom correspondence should be addressed: Box 711, 601 Elmwood Ave., Rochester, NY 14642. Tel.: 585-275-0892; Fax: 585-273-2652; E-mail: Alan_Smrcka@urmc.rochester.edu.

[3] The abbreviations used are: PLC, phosphatidylinositol-specific phospholipase C; AKAP, A kinase anchoring protein; mAKAPβ, muscle-specific AKAP; NRVM, neonatal rat ventricular myocyte; NE, norepinephrine; Iso, isoproterenol; ET-1, endothelin-1; Epac, exchange protein activated by cAMP; IP, inositol phosphate; IP_3, inositol trisphosphate; DAG, diacylglycerol; CamK, calcium calmodulin-dependent kinase; RA, Ras association domain; SR, sarcoplasmic reticulum; SR1, spectrin repeat domain 1; AR, adrenergic receptor; GEF, guanine nucleotide exchange factor; ANF, atrial natriuretic factor.

ular myocyte (NRVM) (19). Surprisingly, in this cell model, we found that PLCε appears to be required for development of cardiac hypertrophy downstream of multiple hypertrophic stimuli, rather than protective.

We also examined the subcellular scaffolding of PLCε that might lead to generation of IP_3 and DAG at specific cellular sites critical for activation of hypertrophic transcriptional mechanisms. A common family of scaffolding molecules in the heart is the protein kinase A anchoring protein (AKAP) family (20, 21). One member of this family that is involved in cytokine- and adrenergic-induced hypertrophy is the alternatively spliced isoform of muscle AKAP (mAKAPβ) expressed exclusively in striated myocytes (22). mAKAPβ binds multiple proteins besides protein kinase A (PKA) including exchange factor activated by cAMP (Epac), adenylate cyclase 5 (23), cAMP-phosphodiesterase 4D3 (PDE4D3), extracellular signal-regulated kinase 5 (ERK5) (22), protein phosphatase 2A (PP2A) (21), and calcineurin (24). mAKAPβ localizes to the nuclear envelope of myocytes, where it is targeted by nesprin-1α (25). It has also been suggested that mAKAPβ scaffolds PKA to ryanodine receptor type 2 (RyR2) in the sarcoplasmic reticulum (SR) (26), but this is controversial. Here we demonstrate that PLCε binds directly to mAKAPβ and that the scaffolding by mAKAPβ is important for the ability of PLCε to regulate cardiomyocyte hypertrophy. This suggests that scaffolding of PLCε to the nuclear envelope by mAKAPβ regulates expression of hypertrophic genes.

EXPERIMENTAL PROCEDURES

Plasmid Constructs—mAKAPβ expression vectors are as described previously (25). All mAKAP vectors are numbered according to mAKAPα because mAKAPβ is identical to mAKAPα 245–2314 (27). PLCε RA1 and PLCε RA2 were in pFLAG3. PLCε ΔCT and PLCε ΔGEF were expressed under the CMV promoter in pCMVscript.

Adenoviral Constructs—Short interfering hairpin RNAs (siRNAs) were designed for targeting mouse, rat, or human PLCε: siRNAPLCε 5, 5′GCCAAATATTCCTACAGCA; RANsiRNA, ACTGTCACAAGTACCTACA (scrambled siRNAPLCε 5). siRNA sequences were subcloned into pShuttle-CMV as in (28), and recombinant viruses were generated following the manufacturer's protocol for the Q-biogene AdEasy adenoviral vector system. Adenoviruses expressing PLCε-RA1 and mAKAP-SR1 were prepared by PCR amplification of the appropriate cDNA fragments and were subcloned into a shuttle vector, under the control of the mouse cytomegalovirus promoter, which also expresses the YFP protein under the control of a separate mouse cytomegalovirus promoter. The shuttle vector was recombined with the parent vector in HEK293 cells to generate adenovirus expressing the PLCε-RA1 or mAKAP-SR1 domain. Recombined virus was amplified in HEK293 cells and purified by CsCl gradient centrifugation. Viral titers were calculated by an immunoreactivity spot assay (29).

Glutathione S-Transferase (GST) Fusion Proteins—GST fusion protein constructs were prepared as described previously (23). BL21 DE3 cells containing pGEX-4T2 plasmids with the indicated regions of mAKAP fused to the C terminus of GST were grown to an optical density (600 nm) of 0.6 followed by induction with 100 μmol/liter isopropyl-1-thio-β-D-galactopyranoside for 16 h at 18 °C in 1 liter of each. Cells were harvested by centrifugation followed by lysis in 30 ml of lysis buffer (10 mmol/liter Tris-Cl, pH 7.5, 150 mmol/liter NaCl, 2 mmol/liter EDTA, and 10 mmol/liter β-mercaptoethanol) + protease inhibitors: 133 μM phenylmethylsulfonyl fluoride, 21 μg/ml 1-chloro-3-tosylamido-7-amino-2-heptanone and L-1-tosylamido-2-phenylethyl chloromethyl ketone, 0.5 μg/ml aprotinin, 0.2 μg/ml leupeptin, 1 μg/ml pepstatin A, 42 μg/ml *p*-tosyl-L-arginine methyl ester, 10 μg/ml soybean trypsin inhibitor, by probe sonication. Nonidet P-40 detergent was added to a final concentration of 1% (v/v), and the samples were incubated on ice for 30 min. Lysates were cleared of insoluble material by centrifugation at 100,000 × *g* for 30 min. Soluble lysates were incubated with 500 μl of glutathione agarose beads (Thermo Fisher) for 2 h at 4 °C. Beads were harvested by centrifugation and washed four times in 20 ml of lysis buffer. Beads bound to GST fragments were analyzed directly by SDS-PAGE and staining with Coomassie Blue as well as by an Amido Black protein assay and stored at 4 °C.

For GST-mAKAP fragment pulldowns, 2 μg of GST fusion protein bound to 25 μl of beads was mixed with 50 ng of purified PLCε in 500 μl of pulldown buffer (10 mmol/liter Tris-Cl, pH 7.5, 150 mmol/liter NaCl, 2 mmol/liter EDTA+). Mixtures were rotated for 2 h at 4 °C. Beads were harvested by centrifugation at 16,000 × *g* at 4 °C for 2 min. After supernatant removal, beads were washed three times with 500 μl of pulldown buffer. Beads were boiled in 30 μl of sample buffer, and 10 μl was loaded on a 7.5% (w/v) SDS-polyacrylamide gel for resolving and Western blotting.

PLCε Purification—His_6-tagged PLCε was purified according to previously published procedures (12).

HEK Cell Culture and Transfection—5×10^5 HEK293 cells cultured in Dulbecco's modified Eagle's medium (DMEM) + 10% (v/v) FBS were plated on poly-D-lysine-coated 6-well plates the day before transfection. 2 μg of DNA was transfected using Lipofectamine Plus reagent (Invitrogen). Proteins were expressed for 48 h prior to harvesting for immunoprecipitation.

Immunoprecipitation, Immunocytochemistry, and Western Blotting—Cells were lysed in 1% (v/v) Nonidet P-40 lysis buffer (10 mmol/liter Tris-Cl, pH 7.5, 50 mmol/liter NaCl, 30 mmol/liter sodium pyrophosphate, 50 mmol/liter NaF, 100 μmol/liter phenylmethylsulfonyl fluoride, and 1% (v/v) Nonidet P-40). After sonication and centrifugation, the supernatant was incubated overnight with anti-Myc antibody (Covance) and Protein G plus agarose beads (Santa Cruz Biotechnology Inc., Santa Cruz, CA) at 4 °C with rocking. Beads were centrifuged for 1 min at 16,000 × *g*, washed twice with 1.0 ml of lysis buffer, washed once with 1.0 ml of phosphate-buffered saline, boiled in 50 μl of 2× SDS sample buffer, and loaded onto a 7.5% (w/v) SDS-polyacrylamide gel. After SDS-PAGE, proteins were transferred to nitrocellulose for 16 h at 25 V followed by immunoblotting for mAKAP (anti-Myc antibody) or PLCε.

Neonatal Cardiac Myocyte Culture, Adenoviral Infection, and Hormone Treatment—NRVMs were isolated and cultured from hearts from 2–3-day-old Sprague-Dawley rats as has been previously described (19) with modifications. Briefly, hearts

were excised, and ventricles were separated and rinsed in Hanks' balanced salt solution prior to digestion with three rounds of collagenase type II (Worthington) in Hanks' balanced salt solution without Ca^{2+} and Mg^{2+}. Cells were collected by centrifugation and resuspended in DMEM containing 10% (v/v) fetal bovine serum (FBS), 100 IU/ml penicillin, 100 μg/ml streptomycin, 2 mmol/liter glutamine, and 2 μg/ml vitamin B-12. Non-myocytes were removed by preplating of the cells for 1 h at 37 °C. The NRVMs were cultured in DMEM as described above containing 10 μmol/liter cytosine arabinoside. 10 μmol/liter cytosine arabinoside was applied for the first 3 days. After overnight incubation, FBS was reduced to 1% (v/v) followed by DMEM lacking serum for at least 24 h. After NRVMs were plated for 6–8 h, adenovirus expressing PLCε siRNA 5, random siRNA, PLCε, PLCε(H1460L), PLCε-RA1, mAKAP-SR1, or YFP as control was added (multiplicity of infection 50) for 4–6 h followed by washing. NRVMs were then cultured in serum-free DMEM medium containing 0.1× insulin-transferrin-selenium. After adenovirus infection for at least 2 days and serum starvation for at least 24 h, 10 nmol/liter ET-1, 10 μmol/liter Iso, 10 μmol/liter norepinephrine (NE), or 10 nmol/liter IGF-1 was added for 48 h to induce hypertrophy.

[^{3}H]Leucine Incorporation—NRVMs were plated in 24-well 0.2% (w/v) gelatin-coated plates at a density of 2×10^5 cells/ml and 500 μl/well. [^{3}H]Leucine (1 μCi/ml) was used to label newly translated proteins for 48 h in the absence or presence of hypertrophic agonist as described above. Cells were washed twice with ice-cold PBS and incubated in 5% (w/v) trichloroacetic acid for 30 min at 4 °C to precipitate the protein. Precipitates were washed twice and solubilized in 0.4 N NaOH for 2 h. Trichloroacetic acid (TCA) precipitable radioactivity was measured by scintillation counting. For analysis, data were pooled from 2–3 independent experiments performed in triplicate.

Cell Area Measurements—NRVMs were plated in 6-well 0.2% (w/v) gelatin-coated plates at a density of 1.0×10^5 cells/ml and 2 ml/well. After hypertrophic agonist treatment, NRVMs were fixed in 4% (w/v) paraformaldehyde, permeabilized with 0.1% (v/v) Nonidet P-40, and immunostained with myocyte marker, sarcomeric α-actinin antibody (Sigma 1:500) in phosphate-buffered saline (PBS) (0.1% Nonidet P-40 (v/v), and bovine serum albumin (BSA) 3% (w/v)) followed by Alexa Fluor 546 (Invitrogen 1:300) in the same solution. Fluorescent images were taken at 20× magnification using an Olympus IX-71 fluorescence microscope. NRVM surface areas were calculated using the NIH ImageJ software from over 400 myocytes from each condition. Data were pooled from 2 independent experiments.

Measurement of PLC Activity in NRVMs—NRVMs were plated in 24-well 0.2% (w/v) gelatin-coated plates at a density of 2×10^5 cells/ml and 500 μl/well. After adenovirus infection for 2 days, NRVMs were labeled for 2 days with [^{3}H]inositol (20 μCi/ml) in inositol-free DMEM supplemented as above. LiCl was added to a final concentration of 100 mM for 10 min at 37 °C. Then agonist was added for 30 min at 37 °C. Total inositol phosphates (IPs) produced were measured as in Ref. 30.

Immunocytochemical Staining—NRVMs were fixed and permeabilized and immunostained as described for cell area measurements using an mAKAPβ antibody (1:500) and an Alexa Fluor 546 secondary antibody. Cells were also treated with 4′,6-diamidino-2-phenylindole (DAPI) to stain nuclei.

Measurement of ANF Levels by Real Time PCR—NRVMs were plated in 6-well 0.2% gelatin-coated plates at a density of 5.0×10^5 cells/ml and 500 μl/well. For real time PCR, total RNA was extracted from NRVM using the RNeasy mini kit (Qiagen). 300 ng was reverse-transcribed with reverse primers to GAPDH and atrial natriuretic factor (ANF) using SuperScript III reverse transcriptase (Invitrogen). Real time PCR was performed on this product on the BioRadCFX96 real time system with a C 1000 thermal cycler using the iQ SYBR Green supermix (Bio-Rad).

The primers used were: ANF, 169-bp PCR product, ANF forward (169), 5′-ATCTGATGGATTTCAAGAACC-3′; ANF reverse (338), 5′-CTCTGAGACGGGTTGACTTC-3′; GAPDH, 260-bp PCR product, GAPDH forward (648), 5′-AAGGTCATCCCAGAGCTGAAC-3′; GAPDH reverse (908), 5′-TCATTGAGAGCAATGCC-3′. ANF values were normalized to GAPDH, and data collected were analyzed using the GraphPad Prism software. Each experiment was performed 2–3 times independently with results from each experiment giving one data point.

Isolation of Nuclei from NRVMs—The protocol was as previously reported except that the fraction containing SR, plasma membrane, and Golgi bodies was not further purified (31).

Statistical Analysis—For the majority of the [^{3}H]leucine incorporation, cell area, real time PCR, and inositol phosphate measurements, significance was calculated by dividing the mean ligand-stimulated response by the unstimulated response for either random or PLCε siRNA treatment to determine fold activation. The difference in fold activation for random siRNA *versus* PLCε siRNA was analyzed for statistical significance using a one-tailed unpaired Student's *t* test. Selected data in Fig. 3*A* were analyzed by one-way analysis of variance with Bonferroni's post test.

RESULTS

PLCε Knockdown in NRVMs Inhibits Endothelin-1-dependent Hypertrophy—We previously established an siRNA protocol for PLCε-specific knockdown in Rat-1 fibroblasts. This siRNA treatment did not affect expression of other PLC isoforms or expression of G proteins, and several siRNA sequences produced similar biological effects (28). We selected the most effective siRNA sequence from those tested (siRNAPLCε 5) that knocked down PLCε by 97% in Rat-1 fibroblasts and created an adenovirus for infection of NRVMs. Supplemental Fig. 1*A* shows RT-PCR analysis of PLCε RNA extracted from NRVMs infected for 3 and 6 days. PLCε mRNA was effectively depleted after 3 days and remained low after 6 days of viral infection. PLCε protein was also depleted after 3 days of viral infection (supplemental Fig. 1*B*), whereas the levels of other PLC isoforms were unaffected by the siRNA treatment (supplemental Fig. 1*C*).

First, we examined the role of PLCε in ET-1-dependent cardiac hypertrophy. ET-1 treatment for 48 h caused a significant increase in three markers of hypertrophy: [^{3}H]leucine incorporation (Fig. 1*A*), cell area (Fig. 1, *B* and *C*), and ANF mRNA (Fig. 1*D*) in random siRNA infected cells, indicating stimulation of

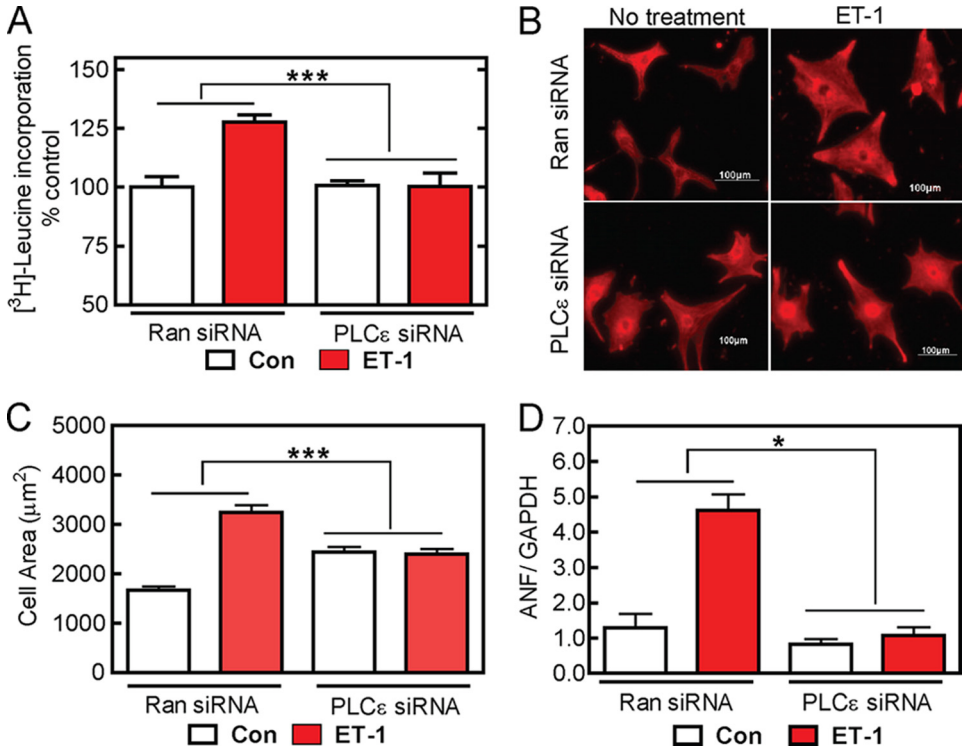

FIGURE 1. **PLCε is required for ET-1-dependent cardiomyocyte hypertrophy.** NRVMs were infected with PLCε-siRNA or random siRNA (*Ran siRNA*) adenoviruses followed by stimulation with 10 nmol/liter ET-1 as described under "Experimental Procedures." *A*, [^{3}H]leucine incorporation was measured as described under "Experimental Procedures." Data are combined results from four separate preparations of myocytes with each experiment performed in triplicate. *Con*, control. *B*, NRVMs were fixed and stained with α-actinin antisera as described under "Experimental Procedures." *Scale bar* is 100 μm. *C*, NRVM surface areas were calculated using the NIH ImageJ software from over 400 myocytes for each condition. Data were pooled from 2 independent experiments. *D*, ANF mRNA was measured by real time PCR and normalized to GAPDH as described under "Experimental Procedures." Data are combined from two different preparations of cells. *Error bars* indicate S.E. *, $p < 0.05$, ***, $p < 0.001$.

the hypertrophic response. Surprisingly, PLCε siRNA blocked ET-1-dependent increases in all hypertrophic markers (Fig. 1, *A–D*), indicating a requirement for PLCε for ET-1-dependent hypertrophy in NRVMs. To show that this result was not due to a nonspecific effect of the PLCε siRNA, we co-expressed PLCε with either a LacZ control or PLCε with a non-coding mutation that provides resistance to the siRNA (PLCε (res)) to replace the endogenously depleted PLCε protein with exogenously expressed PLCε. Leucine incorporation was monitored as a measure of hypertrophy (supplemental Fig. 1*D*). As in Fig. 1*A*, PLCε siRNA suppressed ET-1-induced [^{3}H]leucine incorporation, but co-expression with PLCε (Res) prevented this effect, demonstrating rescue of the hypertrophic response upon re-expression of PLCε in the PLC siRNA background.

Overall, suppression of the hypertrophic response to ET-1 by PLCε depletion was unexpected because it is the opposite of what was observed in the PLCε$^{-/-}$ mice where the loss of PLCε appeared to increase hypertrophy. Regardless of this apparent contradiction, this result was also unexpected because ET-1 is thought to stimulate phosphatidyl inositol hydrolysis through a G_q-dependent mechanism that would not be expected to directly involve PLCε. ET_A receptors can also signal via $G_{12/13}$-Rho-, $G_i/\beta\gamma$-, and G_s-dependent pathways, and it is possible that PLCε is regulated through one of these signaling mechanisms. It was noted that PLCε knockdown alone increased cell area in the absence of stimulation by ET-1, but this appears to be unrelated to the hypertrophic response because the other markers of hypertrophy, ANF mRNA levels and protein synthesis, are not significantly altered by PLCε siRNA treatment in the absence of stimulation by agonist.

PLCε Is a Central Participant in Ligand-dependent Hypertrophic Responses in NRVMs—PLCε has the potential to be regulated by multiple upstream signaling mechanisms. We have extensively characterized a role in cAMP-Epac- and Rap-dependent signaling, and PLCε can respond to multiple G protein-coupled receptor-dependent and receptor tyrosine kinase-dependent pathways through Ras, Rho, Gβγ, or other potential regulatory molecules (13, 16, 17, 32). For this reason, we examined the effects of PLCε knockdown on stimulation of hypertrophy by agonists that signal through distinct cellular mechanisms. Iso likely works through a cAMP-dependent mechanism. NE activates G_q-dependent signaling via stimulation of α1-adrenergic receptors in neonatal myocytes (33). IGF-1 signals via tyrosine phosphorylation and couples to PLCγ (8). Again, PLCε knockdown almost completely inhibited ligand-dependent hypertrophy by all of these agonists (Fig. 2 and supplemental Fig. 2), indicating a central role of PLCε in hypertrophic signaling by diverse hormonal regulatory mechanisms.

To determine whether PLCε overexpression can promote hypertrophy in NRVMs, cells were infected with an adenovirus expressing PLCε under the control of a mouse cytomegalovirus promoter, and [^{3}H]leucine incorporation was measured. PLCε expression alone significantly increased leucine incorporation (Fig. 3*A*), indicating that increasing PLCε expression was sufficient to increase hypertrophy. ET-1 was able to further increase

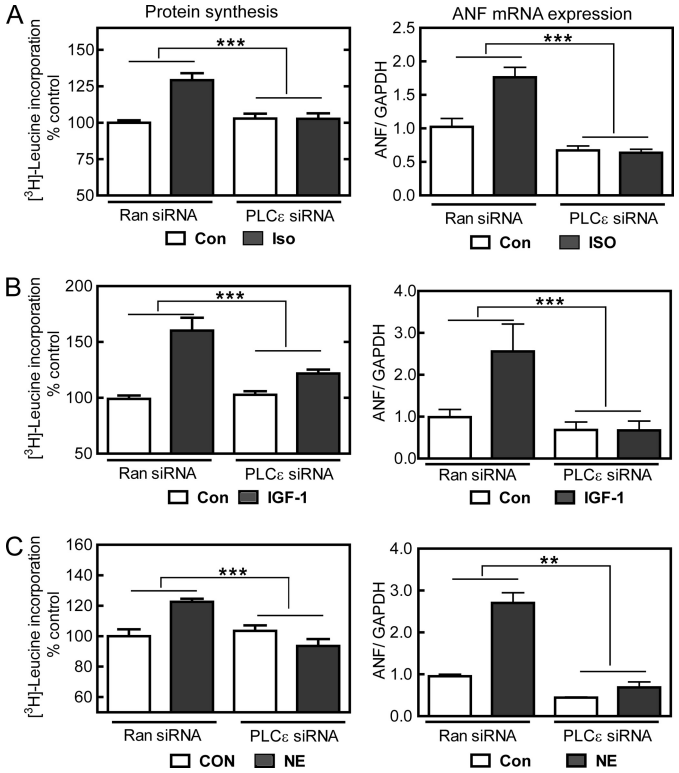

FIGURE 2. **PLCε mediates cardiomyocyte hypertrophy downstream of multiple signaling pathways.** Cells were treated as in Fig. 1 except with 10 μmol/liter Iso (*A*), 10 nmol/liter IGF-1 (*B*), or 10 μmol/liter NE (*C*). [^{3}H]Leucine incorporation and ANF mRNA were measured as in Fig. 1. Data are pooled from three preparations of NRVMs for leucine incorporation performed in triplicate or two preparations of NRVMs for ANF measurement. *Error bars* indicate S.E. **, $p < 0.01$, ***, $p < 0.001$. *Con*, control; *Ran siRNA*, random siRNA.

[^{3}H]leucine incorporation in the context of PLCε overexpression. To determine whether PLCε catalytic activity was required for the PLCε-dependent increase in hypertrophy, we expressed PLCε with a point mutation in the catalytic domain that eliminates PLC hydrolytic activity (PLCε(H1460L)) and measured hypertrophy. Expression of PLCε(H1460L) did not stimulate hypertrophy when compared with the YFP control. Expression of PLCε(H1460L) also suppressed hypertrophy stimulated by ET-1, likely acting in a dominant negative manner (Fig. 3*A*). Adenoviral expression of PLCε and PLCε(H1460L) gives equal levels of PLCε protein in ventricular myocytes (not shown). These data indicate that the products of PLCε catalytic activity are important for the hypertrophic response. To examine the role of PLCε in receptor-driven phosphatidylinositol 4,5-bisphosphate hydrolysis, we knocked down PLCε with siRNA and examined ET-1- and NE-stimulated IP production. PLCε knockdown had no effect on the ability of these agonists to stimulate total IP production (Fig. 3, *B* and *C*). We propose that PLCε activity does not significantly contribute to global cellular IP production either because it is expressed at very low levels, because its localization is restricted, or both. Possible mechanisms for subcellular localization of activity are discussed in depth below. Overall, these data suggest that PLCε is necessary for hypertrophy driven by multiple neurohumoral stimuli and that PLCε activity is sufficient to drive hypertrophic responses.

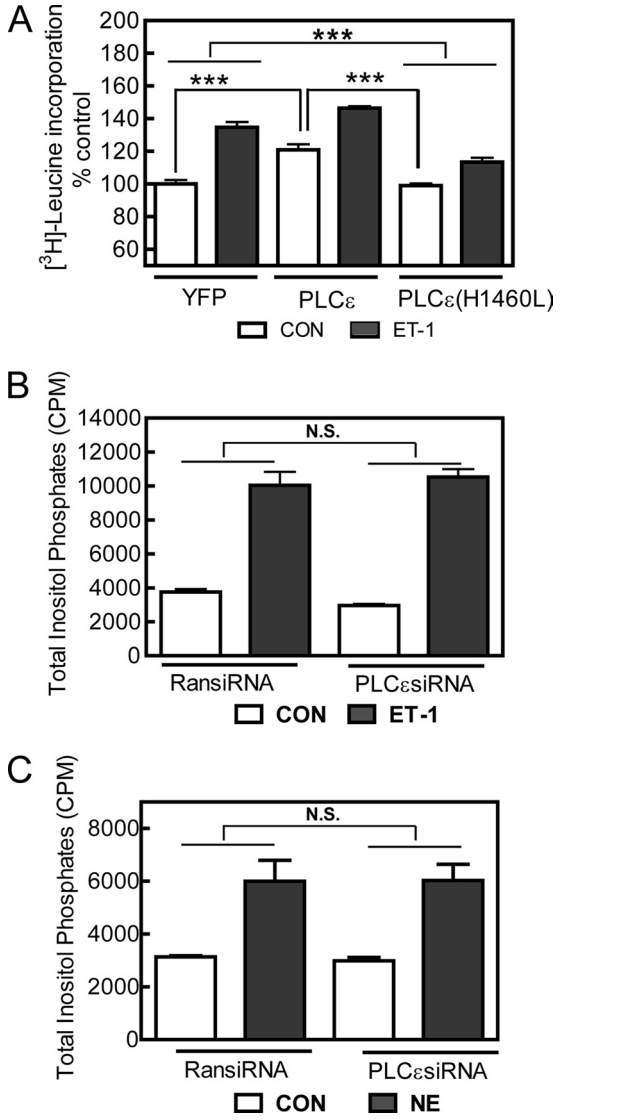

FIGURE 3. **PLCε hydrolytic activity promotes hypertrophy but does not contribute significantly to global IP_3 production in NRVMs.** *A*, NRVMs were infected with adenoviruses expressing either PLCε or catalytically inactive PLCε(H1460L) and treated with or without ET-1 for 48 h. [^{3}H]Leucine incorporation was measured as described under "Experimental Procedures." Data are pooled results from 3 separate experiments performed in triplicate, ***, $p < 0.001$. *Error bars* indicate S.E. *CON*, control. *B* and *C*, total inositol phosphates were measured after a 30-min treatment of NRVMs with or without (*CON*) 100 nM ET-1 (*B*) or 100 μmol/liter NE (*C*). Data are combined results from 2 separate experiments performed in triplicate. *N.S.*, not significant; *RansiRNA*, random siRNA.

mAKAP Binds PLCε in Transfected Cells and in the Heart—Because the data suggest that PLCε may be acting locally to produce its physiological effects and because one of the regulators of PLCε, Epac, scaffolds to mAKAPβ, we tested whether PLCε could interact with mAKAPβ. Myc-mAKAP was co-expressed with PLCε in HEK293 cells followed by immunoprecipitation of mAKAP and immunoblotting for either PLCε or mAKAP (Fig. 4*A*). PLCε was found in Myc-mAKAP immunoprecipitates only when both proteins were expressed. No PLCε immunoreactivity was detected if either PLCε or Myc-mAKAP was absent. To determine whether mAKAPβ and PLCε associate in cardiac tissue, mouse heart lysates were prepared from PLCε$^{+/+}$ and PLCε$^{-/-}$ mice followed by PLCε immunopre-

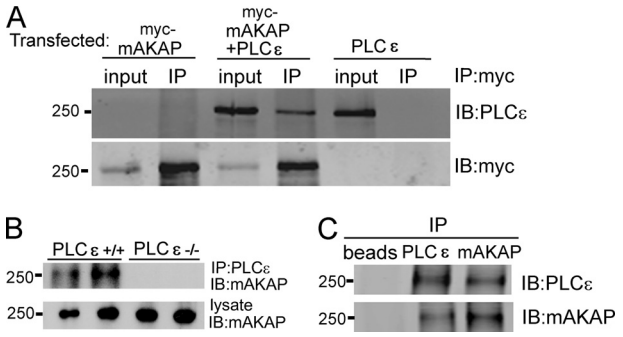

FIGURE 4. **PLCε interacts with mAKAP in transfected HEK293 cells and in native mouse heart tissue.** *A*, HEK293 cells were transfected with Myc-mAKAP alone, PLCε alone, or PLCε with Myc-mAKAP. Cells were lysed and immunoprecipitated (*IP*) with an anti-Myc specific antibody. Lysates were Western blotted (*IB*) for either PLCε or Myc. *B*, Nonidet P40 soluble lysates were prepared from hearts isolated from PLCε$^{+/+}$ mice, or PLCε$^{-/-}$ mice as a control, immunoprecipitated with anti PLCε antibodies, and immunoblotted for mAKAPβ. *C*, Nonidet P40 lysates from PLCε$^{+/+}$ mice as in *B* were immunoprecipitated with either anti-mAKAP or PLCε antibodies and immunoblotted as indicated. Lysates were directly blotted with mAKAPβ antisera as loading controls. Each experiment was repeated at least 3 times with similar results.

cipitation and immunoblotting for mAKAPβ (Fig. 4*B*). Lysates from PLCε$^{-/-}$ mouse hearts were used as controls to confirm that bands observed from the immunoprecipitation were the result of association with immunoprecipitated PLCε and not nonspecific immunoprecipitation. mAKAPβ immunoreactivity was detected in immunoprecipitates from PLCε$^{+/+}$ heart lysates but not in immunoprecipitates from PLCε$^{-/-}$ hearts, indicating that mAKAPβ associates with PLCε in native cardiac tissue. PLCε also co-precipitated with mAKAPβ when mouse heart extracts were immunoprecipitated with mAKAPβ antisera (Fig. 4*C*, *lane 3*).

Direct Binding of PLCε to mAKAPβ and Mapping of the Binding Site on the Scaffold—To test for a direct interaction between PLCε and mAKAP and to map the PLCε binding regions on mAKAP, GST fusion proteins corresponding to different domains of the scaffold were purified (Fig. 5*A*) and tested for binding to purified full-length PLCε. First, fragments of mAKAP indicated in Fig. 5*A* were fused to GST, purified, and tested for binding to purified full-length PLCε. A fragment corresponding to mAKAP 586–1286 consistently bound specifically to PLCε, demonstrating direct binding of PLCε to mAKAP and localization to this region of mAKAP (Fig. 5*B*). The 586–1286 domain contains three spectrin repeat-like domains, the third of which is involved in interactions with nesprin-1α that localizes mAKAPβ to the nuclear envelope in cardiac myocytes (25). To further dissect these domains, fragments comprising each of the different repeats were fused to GST, purified, and tested for PLCε binding. Of these fragments, GST-615–915 binds the strongest, with fragment GST-1065–1240 also showing some binding (Fig. 5*C*). The 615–915 fragment of mAKAP contains the first of the three spectrin repeat-like structures (amino acids 772–882). Spectrin repeat-like domains contain two conserved tryptophans (Trp-793 and Trp-867 in the mAKAP first spectrin repeat-like domain) that are important for thermodynamic stability. Mutation of analogous Trp residues to proline in the third spectrin repeat-like domain disrupted interactions between mAKAP and nesprin-1α. Trp-793 was mutated to proline in the mAKAP spectrin repeat-like domain 1, and binding of this mutant protein fused to GST to purified PLCε was examined (Fig. 5*D*). This mutation strongly decreased binding of PLCε to this domain, confirming that PLCε binds to the first spectrin repeat-like domain in mAKAP.

Identification of PLCε Functional Domains Required for mAKAP Interactions—To identify specific domains in PLCε that mediate mAKAP binding, PLCε truncated at the C terminus (ΔCT) to delete the Ras association (RA) domains or PLCε with a GEF domain deletion (ΔGEF) was co-expressed with Myc-mAKAP in HEK293 cells (Fig. 6*A*). The ΔCT mutant was unable to interact with mAKAP in co-immunoprecipitation assays, whereas the interaction was unaffected by the ΔGEF mutation (Fig. 6*B*). Next, either the PLCε-RA1 or the PLCε-RA2 domains were expressed with Myc-mAKAP followed by Myc-mAKAP immunoprecipitation. Both PLCε-RA1 and PLCε-RA2 independently bound to co-expressed mAKAP (Fig. 6*C*). These data indicate that the RA domains are necessary and sufficient for binding of PLCε to mAKAP. Given that the RA domains are important for Rap and Ras interactions, we determined whether activated RapG12V or RasG12V altered PLCε-mAKAP binding in transfected cells. Expression of activated Rap or Ras did not affect PLCε-mAKAP co-immunoprecipitation (data not shown).

Disruption of mAKAP-PLCε Binding by Expression of PLCε RA1 or mAKAP-SR1—To determine whether expression of PLCε-RA1 or mAKAP-SR1 could compete for PLCε binding to mAKAP, mAKAP and PLCε were co-expressed in HEK293 cells, plus or minus co-expression of PLCε-RA1 or mAKAP-SR1 domains. Myc-mAKAP protein complexes were immunoprecipitated with Myc antibodies and immunoblotted for PLCε. PLCε co-immunoprecipitated with mAKAP, but expression of either PLCε-RA1 or mAKAP-SR1 prevented mAKAP-PLCε co-immunoprecipitation (Fig. 7*A*). To test whether PLCε-RA1 or mAKAP-SR1 can disrupt endogenous mAKAP-PLCε signaling complexes in NRVMs, NRVMs were infected with adenoviruses expressing either domain followed by immunoprecipitation of mAKAP and immunoblotting for PLCε. PLCε co-immunoprecipitated with mAKAP when YFP was expressed as a control (Fig. 7*B*), although the complex was difficult to detect. In general, endogenous PLCε is difficult to detect and has to be enriched by direct IP from most tissues to enable adequate detection by immunoblotting. Nevertheless, expression of either PLCε-RA1 or mAKAP-SR1 in NRVMs significantly reduced the association of PLCε with mAKAP immunoprecipitates (Fig. 7*B*), indicating that expression of either of these domains disrupts endogenous mAKAPβ-PLCε complexes in NRVMs.

To confirm the location of endogenous mAKAPβ in NRVMs, isolated myocytes were fixed and stained with mAKAP antibody (data not shown). As reported previously, there was a very strong perinuclear staining of mAKAP (25). Reliable detection of PLCε by immunocytochemistry was not possible, likely due to its low abundance coupled with nonspecific background staining with PLCε antibodies. Given the interaction with mAKAPβ and the predominant perinuclear localization of mAKAP, it is likely that PLCε interaction with

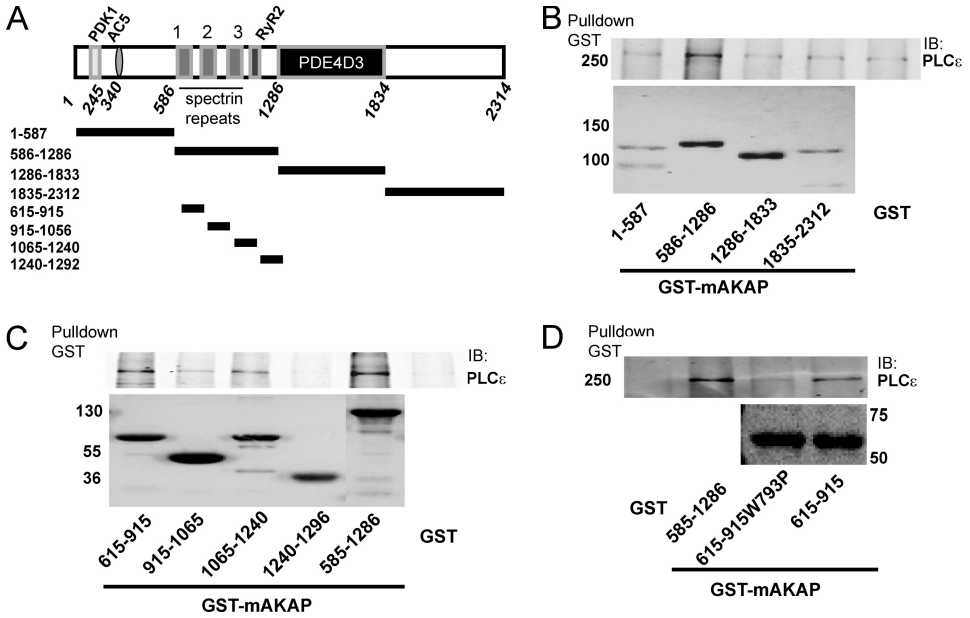

FIGURE 5. **Direct binding of PLCε to mAKAP subdomains.** *A*, diagram of mAKAP showing defined domains for binding PDK1, AC5, RyR2, and PDE4D3, and below, showing the regions that were cloned as GST fusion proteins. *B*, GST fusion proteins corresponding to the larger fragments shown in *A* were tested for binding to purified PLCε. The *top panel* is a Western blot (*IB*) for PLCε after pulldown with the indicated GST fragments. The *bottom panel* is a Coomassie Blue-stained gel of the purified GST fusion proteins. *C*, GST fusion proteins corresponding to the smaller subfragments of the 586–1286 binding domain defined in *B* were tested for binding to purified PLCε. The *top panel* is a Western blot for PLCε after pulldown with the indicated GST fragments. The *bottom panel* is a Coomassie Blue-stained gel of the purified GST fusion proteins. *D*, the 615–915 fragment defined in *C* was mutated by site-directed mutagenesis (W793P), purified, and tested for binding to purified PLCε. The *top panel* is a Western blot for PLCε after pulldown with the indicated GST fragments. The *bottom panel* is a Coomassie Blue-stained gel of the purified GST fusion proteins. Each experiment was repeated at least 3 times with similar results.

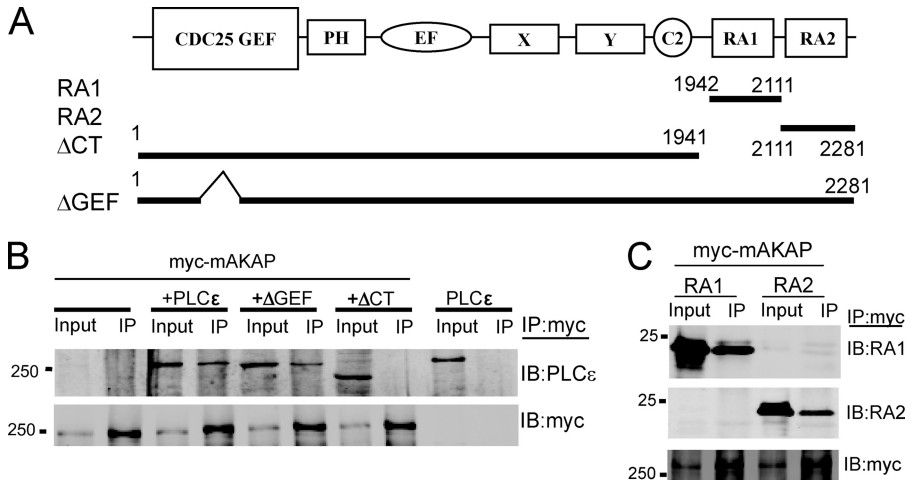

FIGURE 6. **The RA domains of PLCε bind to mAKAP.** *A*, domain structure of PLCε showing the CDC25 guanine nucleotide exchange factor domain (*CDC25 GEF*), a putative pleckstrin homology domain (*PH*), the EF hand domain, the X and Y catalytic domain, the C2 lipid binding domain, and the RA homology domains. Only RA2 binds Ras. *B*, Myc-mAKAP alone or with the indicated PLCε constructs was cotransfected into HEK293 cells, and Myc-mAKAP was immunoprecipitated (*IP*) followed by immunoblotting (*IB*) with anti-PLCε antibody (*top panel*) or Myc antibody as a control (*bottom panel*). *C*, Myc-mAKAP was cotransfected with either PLCε-RA1 or PLCε-RA2 domains. Cells were lysed and immunoprecipitated with anti-Myc antibodies and immunoblotted with the antibodies indicated on the *right*. Each experiment was repeated at least 3 times with similar results.

mAKAPβ localizes some of the PLCε pool to the perinuclear region of the cell. To confirm the nuclear localization of PLCε, NRVMs were fractionated to isolate nuclei and immunoblotted for PLCε. PLCε was significantly enriched in the nuclear fraction when compared with whole cell NRVM lysate, consistent with association with nuclear-bound mAKAP. Nuclear enrichment was confirmed by measuring the enrichment of the nuclear protein LAP-2 and the mAKAPβ. Both proteins were greatly enriched relative to the whole cell NRVM lysates. To confirm that the nuclei were free of SR, the lysates were probed for calsequestrin, which was enriched in an SR fraction but was absent from the nuclear fraction.

mAKAPβ spectrin repeat domain 3, but not repeats 1 or 2, has been shown to mediate interactions with nesprin-1α, which localizes mAKAP to the perinuclear region (25) of cardiac myocytes. Nevertheless, because PLCε interacts with spectrin repeat domain 1, we tested whether expression of either PLCε-RA1 or mAKAP-SR1 disrupted perinuclear localization of mAKAPβ in NRVMs. Neither domain altered the localization of mAKAPβ as assessed by immunocytochemistry of NRVMs

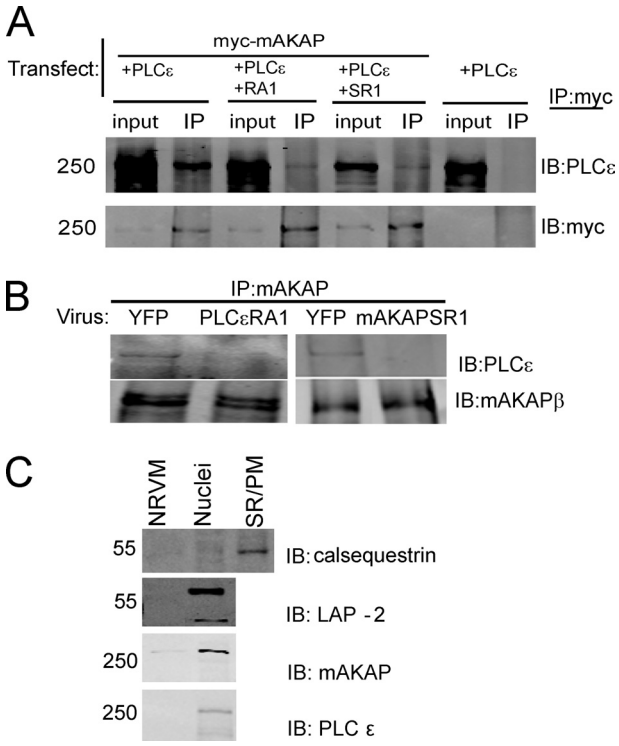

FIGURE 7. **The PLCε-RA1 and mAKAP-SR1 domains compete for mAKAP-PLCε interactions.** *A*, PLCε and Myc-mAKAP were cotransfected (*Transfect.*) into HEK393 cells in the presence or absence of PLCε-RA1 or mAKAP-SR1 domains. Myc-mAKAP was immunoprecipitated (*IP*) and Western blotted (*IB*) for PLCε (*top panel*) or Myc (*bottom panel*). Each experiment was repeated at least 3 times with similar results. *B*, NRVMs were infected with adenoviruses expressing YFP, PLCε-RA1, or mAKAP-SR1 for 48 h. Lysates were prepared (1 mg of protein, PLCε-RA1-infected cells, or 2 mg of protein, mAKAP-SR1-infected cells), and mAKAPβ was immunoprecipitated. Immunoprecipitates were immunoblotted for either PLCε or mAKAPβ. This experiment was repeated twice. *C*, NRVMs were fractionated to isolate nuclei and 10 μg of protein was analyzed by Western blotting. *SR/PM*, sarcoplasmic reticulum/plasma membrane.

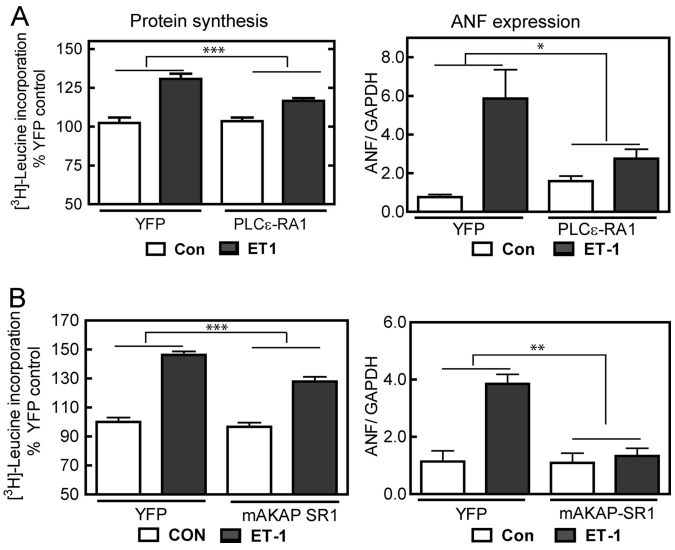

FIGURE 8. **PLCε-RA1 or mAKAP-SR1 expression in neonatal cardiac myocytes inhibits development of cardiac hypertrophy in response to ET-1 treatment.** Cells infected with adenovirus expressing either PLCε-RA1 or YFP (*A*) or mAKAP-SR1 or YFP (*B*) were treated with or without (*CON*) 10 nmol/liter ET-1 for 48 h followed by measurement of [^{3}H]leucine incorporation or ANF mRNA. Data were normalized to YFP with no ET-1 treatment (*CON*). Data are the combined results from 3 separate experiments performed in triplicate for leucine incorporation or 2 separate experiments for ANF mRNA. *Error bars* indicate S.E. *, $p < 0.05$, **, $p < 0.01$, ***, $p < 0.001$.

(supplemental Fig. 3), indicating that these domains effectively disrupt endogenous mAKAPβ-PLCε interactions without influencing mAKAPβ localization to the nuclear envelope. Thus, expression of PLCε-RA1 or mAKAP-SR1 likely disrupts PLCε localization at the nuclear envelope, while leaving the mAKAPβ scaffold itself undisturbed.

Importance of PLCε Scaffolding to mAKAP in Cardiomyocyte Function—We have shown that PLCε is an important central mediator of hypertrophy and that it is scaffolded to mAKAPβ, which we have also shown to be important for cardiac myocyte hypertrophy (16). To establish the functional relevance of mAKAPβ-PLCε complexes, we tested whether mAKAPβ-PLCε binding was required for the hypertrophy of NRVMs. NRVMs were infected with an adenovirus expressing either PLCε-RA1 or mAKAP-SR1 to disrupt PLCε-mAKAP binding followed by treatment with 10 nM ET-1 for 48 h. Expression of either PLCε-RA1 or mAKAP-SR1 significantly blunted ET-1-dependent increases in [^{3}H]leucine incorporation and ANF mRNA expression (Fig. 8, *A* and *B*). PLCε-RA1 is related to Ras binding domains but does not bind Ras or Rap (34). Nevertheless, to be sure that PLCε-RA1 was not inhibiting hypertrophy by blocking Ras or Rap signaling, we measured IGF-1-stimulated ERK phosphorylation, in the presence or absence of PLCε-RA1 expression. The IGF-1-stimulated increase in ERK1/2 phosphorylation in NRVMs was not affected by expression of PLCε-RA1 (data not shown), indicating that these proteins do not globally interfere with Ras signaling. That two independent approaches to disrupting mAKAPβ-PLCε complexes, using two different binding domains from two different proteins, both significantly inhibited ET-1-dependent hypertrophy strongly suggests that scaffolding of PLCε to mAKAPβ is required for hypertrophic responses mediated by ET-1. PLCε-RA1 expression in NRVMs also significantly inhibited [^{3}H]leucine incorporation in response to Iso, NE, and IGF-1, indicating a general role for nuclear scaffolding of PLCε (supplemental Fig. 4).

DISCUSSION

Here we demonstrate that PLCε plays a central role in mediating hypertrophy downstream of multiple agonists and that subcellular scaffolding of PLCε to mAKAPβ, likely at the nuclear envelope, is critical for this process. Mechanistically, the upstream pathways that regulate PLCε for these hypertrophic responses remain to be defined in NRVMs. Possible mechanisms for activation include $G_{12/13}$-dependent Rho pathways, cAMP-Epac pathways, and Ras pathways. ET_A receptors can activate $G_{12/13}$, IGF-1 receptors can activate Ras, and βAR can activate cAMP-Epac-Rap, all of which are potential PLCε regulators in NRVMs. α1-Adrenergic receptors signal primarily through G_q, which would not activate PLCε, but G_q activation can lead to activation of Rho and Ras pathways that could regulate PLCε activity. That PLCε can respond to such diverse signals ideally positions it to be a central integrator of multiple hormonal signals that impinge on the cardiac myocytes during physiologic and pathological stimulation.

Regardless of the mechanism for activation, the catalytic activity of PLCε is required for hypertrophy because expression of a catalytically inactive form of PLCε does not stimulate hypertrophy and blocks development of ET-1-dependent hypertrophy. PLC activity results in the production of two second messengers, DAG and IP_3, and roles for both of these molecules have been suggested in hypertrophy. Nevertheless, the data show that PLCε is not responsible for the majority of global IP_3 generation downstream of ET_A or α1AR. An attractive hypothesis to explain this is that PLCε scaffolded to mAKAPβ at the nuclear envelope generates IP_3 and DAG locally to regulate nuclear Ca^{2+} or PKC signals without significantly contributing to the pool of total IPs. In ventricular myocytes, IP_3 receptors are localized primarily to the nuclear envelope and release a pool of nuclear calcium distinct from that involved in calcium-induced calcium release (35, 36). This nuclear calcium pool has been implicated in regulating hypertrophic gene expression through two pathways: (i) activation of nuclear CamKII leading to phosphorylation of histone deacetylase 5 (HDAC5) and derepression of myocyte enhancer factor (MEF)-dependent transcription; and (ii) activation of calcineurin-dependent dephosphorylation of nuclear factor of activated T-cells (NFAT) leading to increased nuclear factor of activated T-cell-dependent transcription. Additionally, PKC activation has been implicated in hypertrophy, and PKC-PKD-dependent phosphorylation of HDAC leads to export of HDAC5 from the nucleus (37). PLCε could be involved in the local generation of either IP_3 or DAG at the nuclear envelope necessary for these processes.

The PLC isoform responsible for the majority of IP_3 production downstream of G_q-coupled receptors has been suggested to be PLCβ because the major known target of $G\alpha_q$ is PLCβ (6, 38), although $G\alpha_q$ can also regulate Rho activation through direct stimulation of RhoGEFs (39). Data directly implicating PLCβ in cardiac hypertrophy have been lacking until recently. These new data show that PLCβ1b overexpression increases NRVM hypertrophy and that inhibition of PLCβ1b sarcolemmal membrane association can inhibit α1AR-dependent hypertrophy (9). Our published results in astrocytes (17) and fibroblasts (28) indicate that surprisingly, many G_q-coupled receptors generate significant accumulation of total IPs through PLCε, suggesting the possibility that some portion of hypertrophy driven through G_q-linked receptors could be downstream of PLCε activation. Nevertheless, the bulk of IP_3 generation in NRVMs does not appear to involve PLCε and is likely PLCβ-driven, suggesting that PLCε-dependent local phosphatidylinositol 4,5-bisphosphate hydrolysis, distinct from the bulk IP pool, is required for hypertrophic responses. It is possible that hypertrophy in response to ET-1 and NE is both PLCβ1b-dependent and PLCε-dependent and that two distinct pools of IP_3 and/or DAG are required for the hypertrophic response.

We previously reported that PLCε activity is important for CamKII-dependent phosphorylation of Ryr2 and regulation of cardiac Ca^{2+} cycling (41). Based on this observation, we predict that mAKAPβ scaffolded PLCε represents a pool of PLCε that is distinct from a separately scaffolded pool that regulates RyR2. mAKAPβ has been reported to bind to RyR2 (26), but this is at odds with the observation that the majority of mAKAPβ is found at the nuclear envelope, whereas the bulk of RyR2 protein is in the SR. Nevertheless, it remains possible that a small pool of mAKAPβ can scaffold PLCε to Ryr2. This hypothesis remains to be investigated.

Our data demonstrating a requirement for PLCε in hormone-regulated hypertrophic responses contrast with our previously reported *in vivo* observation that global PLCε$^{-/-}$ mice are more sensitive to the development of hypertrophy in response to chronic Iso treatment (18). A possible explanation for the difference in the cellular and *in vivo* data is that in the context of development of the PLCε$^{-/-}$ mice, compensatory pathways were up-regulated that sensitized mice to hypertrophy. In particular, we found that CamKII phosphorylation is basally increased in PLCε$^{-/-}$ mice (supplemental Fig. 5), which could lead to enhanced sensitivity to stress-induced hypertrophy because CamKII activation has been shown to be prohypertrophic (40). CamKII activation is not elevated in PLCε siRNA-treated myocytes (data not shown). It is not unusual for compensatory pathways to be up- or down-regulated in global knock-out mice where the gene product is lost from birth. This suggests that our previous conclusion from global PLCε$^{-/-}$ mice suggesting a protective role for PLCε was incorrect. Analysis of mice with cardiac myocyte-specific, acute PLCε knockdown would help to resolve this discrepancy.

Overall, these data demonstrate that PLCε plays a central role in mediating hypertrophy in response to multiple neurohumoral stimuli and that scaffolding to mAKAPβ is critical for this. The human heart is exposed to multiple hormonal inputs during the development of heart failure. PLCε represents a potentially interesting therapeutic target as a central integrator of these inputs, possibly allowing for more efficacious treatment of heart failure. Because PLCε plays an important role in the CNS, pancreas, and kidney as well as other tissues, targeting PLCε activity directly might not be desirable. Development of an approach that could specifically interfere with PLCε-mAKAPβ interactions could provide a more selective approach to targeting PLCε and its role in hypertrophy.

Acknowledgments—We thank the Dr. Shey-Shing Sheu laboratory for assistance with preparation of NRVMs and Dr. Tzong-Jen for sharing neonatal rats.

REFERENCES

1. Knowlton, K. U., Michel, M. C., Itani, M., Shubeita, H. E., Ishihara, K., Brown, J. H., and Chien, K. R. (1993) *J. Biol. Chem.* **268,** 15374–15380
2. Barki-Harrington, L., Perrino, C., and Rockman, H. A. (2004) *Cardiovasc. Res.* **63,** 391–402
3. Shubeita, H. E., McDonough, P. M., Harris, A. N., Knowlton, K. U., Glembotski, C. C., Brown, J. H., and Chien, K. R. (1990) *J. Biol. Chem.* **265,** 20555–20562
4. Rhee, S. G. (2001) *Annu. Rev. Biochem.* **70,** 281–312
5. Adams, J. W., Sakata, Y., Davis, M. G., Sah, V. P., Wang, Y., Liggett, S. B., Chien, K. R., Brown, J. H., and Dorn, G. W., 2nd (1998) *Proc. Natl. Acad. Sci. U.S.A.* **95,** 10140–10145
6. Smrcka, A. V., Hepler, J. R., Brown, K. O., and Sternweis, P. C. (1991) *Science* **251,** 804–807
7. Bers, D. M. (2008) *Annu. Rev. Physiol.* **70,** 23–49
8. Foncea, R., Andersson, M., Ketterman, A., Blakesley, V., Sapag-Hagar, M., Sugden, P. H., LeRoith, D., and Lavandero, S. (1997) *J. Biol. Chem.* **272,**

19115–19124
9. Filtz, T. M., Grubb, D. R., McLeod-Dryden, T. J., Luo, J., and Woodcock, E. A. (2009) *FASEB J.* **23,** 3564–3570
10. Singer, W. D., Brown, H. A., and Sternweis, P. C. (1997) *Ann. Rev. Biochem.* **66,** 475–509
11. Harden, T. K., and Sondek, J. (2006) *Annu. Rev. Pharmacol. Toxicol.* **46,** 355–379
12. Kelley, G. G., Reks, S. E., Ondrako, J. M., and Smrcka, A. V. (2001) *EMBO J.* **20,** 743–754
13. Kelley, G. G., Reks, S. E., and Smrcka, A. V. (2004) *Biochem. J.* **378,** 129–139
14. Lopez, I., Mak, E. C., Ding, J., Hamm, H. E., and Lomasney, J. W. (2001) *J. Biol. Chem.* **276,** 2758–2765
15. Song, C., Hu, C. D., Masago, M., Kariyai, K., Yamawaki-Kataoka, Y., Shibatohge, M., Wu, D., Satoh, T., and Kataoka, T. (2001) *J. Biol. Chem.* **276,** 2752–2757
16. Wing, M. R., Houston, D., Kelley, G. G., Der, C. J., Siderovski, D. P., and Harden, T. K. (2001) *J. Biol. Chem.* **276,** 48257–48261
17. Citro, S., Malik, S., Oestreich, E. A., Radeff-Huang, J., Kelley, G. G., Smrcka, A. V., and Brown, J. H. (2007) *Proc. Natl. Acad. Sci. U.S.A.* **104,** 15543–15548
18. Wang, H., Oestreich, E. A., Maekawa, N., Bullard, T. A., Vikstrom, K. L., Dirksen, R. T., Kelley, G. G., Blaxall, B. C., and Smrcka, A. V. (2005) *Circ. Res.* **97,** 1305–1313
19. Simpson, P., McGrath, A., and Savion, S. (1982) *Circ. Res.* **51,** 787–801
20. Scott, J. D., and Santana, L. F. (2010) *Circulation* **121,** 1264–1271
21. Dodge-Kafka, K. L., Langeberg, L., and Scott, J. D. (2006) *Circ. Res.* **98,** 993–1001
22. Dodge-Kafka, K. L., Soughayer, J., Pare, G. C., Carlisle Michel, J. J., Langeberg, L. K., Kapiloff, M. S., and Scott, J. D. (2005) *Nature* **437,** 574–578
23. Kapiloff, M. S., Piggott, L. A., Sadana, R., Li, J., Heredia, L. A., Henson, E., Efendiev, R., and Dessauer, C. W. (2009) *J. Biol. Chem.* **284,** 23540–23546
24. Pare, G. C., Bauman, A. L., McHenry, M., Michel, J. J., Dodge-Kafka, K. L., and Kapiloff, M. S. (2005) *J. Cell Sci.* **118,** 5637–5646
25. Pare, G. C., Easlick, J. L., Mislow, J. M., McNally, E. M., and Kapiloff, M. S. (2005) *Exp. Cell Res.* **303,** 388–399
26. Marx, S. O., Reiken, S., Hisamatsu, Y., Jayaraman, T., Burkhoff, D., Rosemblit, N., and Marks, A. R. (2000) *Cell* **101,** 365–376
27. Michel, J. J., Townley, I. K., Dodge-Kafka, K. L., Zhang, F., Kapiloff, M. S., and Scott, J. D. (2005) *Mol. Cell* **20,** 661–672
28. Kelley, G. G., Kaproth-Joslin, K. A., Reks, S. E., Smrcka, A. V., and Wojcikiewicz, R. J. H. (2006) *J. Biol. Chem.* **281,** 2639–2648
29. Duale, H., Kasparov, S., Paton, J. F., and Teschemacher, A. G. (2005) *Exp. Physiol.* **90,** 71–78
30. Malik, S., Ghosh, M., Bonacci, T. M., Tall, G. G., and Smrcka, A. V. (2005) *Mol. Pharmacol.* **68,** 129–136
31. Kapiloff, M. S., Jackson, N., and Airhart, N. (2001) *J. Cell Sci.* **114,** 3167–3176
32. Wing, M. R., Snyder, J. T., Sondek, J., and Harden, T. K. (2003) *J. Biol. Chem.* **278,** 41253–41258
33. Simpson, P. (1985) *Circ. Res.* **56,** 884–894
34. Bunney, T. D., Harris, R., Gandarillas, N. L., Josephs, M. B., Roe, S. M., Sorli, S. C., Paterson, H. F., Rodrigues-Lima, F., Esposito, D., Ponting, C. P., Gierschik, P., Pearl, L. H., Driscoll, P. C., and Katan, M. (2006) *Mol. Cell* **21,** 495–507
35. Higazi, D. R., Fearnley, C. J., Drawnel, F. M., Talasila, A., Corps, E. M., Ritter, O., McDonald, F., Mikoshiba, K., Bootman, M. D., and Roderick, H. L. (2009) *Mol. Cell* **33,** 472–482
36. Wu, X., Zhang, T., Bossuyt, J., Li, X., McKinsey, T. A., Dedman, J. R., Olson, E. N., Chen, J., Brown, J. H., and Bers, D. M. (2006) *J. Clin. Invest.* **116,** 675–682
37. Vega, R. B., Harrison, B. C., Meadows, E., Roberts, C. R., Papst, P. J., Olson, E. N., and McKinsey, T. A. (2004) *Mol. Cell. Biol.* **24,** 8374–8385
38. Smrcka, A. V., and Sternweis, P. C. (1993) *J. Biol. Chem.* **268,** 9667–9674
39. Aittaleb, M., Boguth, C. A., and Tesmer, J. J. G. (2010) *Mol. Pharmacol.* **77,** 111–125
40. Zhang, T., and Brown, J. H. (2004) *Cardiovasc. Res.* **63,** 476–486
41. Oestreich, E. A., Malik, S., Goonasekera, S. A., Blaxall, B. C., Kelley, G. G., Dirksen, R. T., and Smrcka, A. V. (2009) *J. Biol. Chem.* **284,** 1514–1522